Flora 337 (2026) 152945

Contents lists available at ScienceDirect

Flora

journal homepage: www.elsevier.com/locate/flora

Evolutionary relationships and genetic structure in Mediterranean *Hypericum* sect. *Adenosepalum* with focus on *H. scruglii*

Veronica Malavasi [a], Núria Beltran-Sanz [a], Caterina Angela Dettori [b], Olga De Castro [c,d,e,*], Gianluigi Bacchetta [b]

[a] Department of Botany, Charles University, Benátská 2, Praha 2. CZ-12800, Czech Republic
[b] Department of Life and Environmental Science, Center for Conservation of Biodiversity (CCB), University of Cagliari, V.le Sant' Ignazio da Laconi, 13, 09123 Cagliari, Italy
[c] Department of Biology, University of Naples Federico II, Via Cinthia, 80126 Naples, Italy
[d] Botanical Garden, University of Naples Federico II, Via Foria 223, 80139 Naples, Italy
[e] ACUF, The Algal Collection at the University of Naples Federico II, Via Cinthia, 80126 Naples, Italy

ARTICLE INFO

Edited by Christoph Oberprieler

Keywords:
Hypericaceae
Mediterranean endemics
ITS
Networks
Phylogeography
Plastid markers

ABSTRACT

Understanding the evolutionary relationships and genetic structure within Mediterranean plant lineages is essential for both systematic and conservation. The genus *Hypericum* (Hypericaceae) presents an ideal model system due to its ecological versatility, pharmacological relevance, and remarkable diversity across biodiversity hotspots. Yet, the placement of Mediterranean endemics remains poorly resolved. In this study, we investigated phylogeographic patterns and genetic differentiation among three species of section *Adenosepalum*: the Sardinian endemic *H. scruglii*, and the more widespread *H. tomentosum* and *H. pubescens*. A multilocus dataset comprising nuclear ribosomal cistron (ITS1, 5.8S and ITS2) and two plastid intergenic spacers [*ycf*6-*psb*M and *trn*S$^{(GCU)}$–*trn*G$^{(UCC)}$] was generated from 71 individuals across 17 populations spanning Italy, Spain, France, and Malta. Phylogenetic reconstructions and phylogeographical network analyses were combined to elucidate evolutionary relationships. Congruence testing revealed significant topological incongruence between nuclear and plastid datasets, suggesting complex evolutionary histories involving incomplete lineage sorting and potential historical gene flow. A combination of ribotype and haplotype network analyses revealed distinct geographic clustering, with *H. scruglii* exhibiting three private plastid haplotypes restricted to Sardinia, while *H. pubescens* and *H. tomentosum* showed broader but non-overlapping ribotype sets. Population-level analysis confirmed higher genetic differentiation in plastid markers ($Fst > 0.6$) than in nuclear markers ($Fst < 0.4$), supporting a scenario of recent Mediterranean diversification with restricted gene flow. Overall, our results provide robust molecular evidence for the taxonomic distinctiveness of *H. scruglii* and contribute to a refined phylogeographic framework for Mediterranean *Hypericum* section *Adenosepalum*, with direct implications for conservation prioritization of insular endemics.

1. Introduction

The Mediterranean Basin, recognized as one of the world's biodiversity mega hotspots, harbors exceptional levels of plant endemism, particularly among insular floras (Bacchetta et al., 2012; Cañadas et al., 2014). Within this context, the genus *Hypericum* L. (Hypericaceae) represents a compelling model for investigating evolutionary processes. The genus comprises approximately 500 species (Robson, 1981, 2003, 2006, 2016; Crockett and Robson, 2011) with a predominantly temperate and montane tropical distribution across all continents except Antarctica (Nürk et al., 2013). The Mediterranean Basin, as part of this global distribution, hosts a significant portion of the genus's diversity and exhibits particularly high rates of endemism, making it an ideal system for studying evolutionary dynamics in island and continental settings.

The genus is characterized by remarkable ecological versatility and pharmacological significance, with many species producing bioactive compounds such as hypericin and hyperforin that have attracted considerable scientific and commercial interest (Kitanov, 2001; Allaw et al., 2020; Kalcev et al., 2021; Al-Khayri et al., 2024).

* Corresponding author.
E-mail address: odecastr@unina.it (O. De Castro).

https://doi.org/10.1016/j.flora.2026.152945
Received 26 September 2025; Received in revised form 10 February 2026; Accepted 11 February 2026
Available online 13 February 2026

In the last few decades, molecular phylogenetic studies have substantially advanced our understanding of *Hypericum* systematics and evolution. The analyses by Nürk et al. (2013, 2015) and Meseguer et al. (2013) established a robust phylogenetic framework for the genus, revealing complex patterns of diversification and biogeographic history, including significant cytonuclear incongruence at deeper nodes within the family. However, several Mediterranean lineages, particularly insular endemics, remain underrepresented in molecular datasets, limiting our understanding of regional evolutionary processes and hampering effective conservation strategies. To address these gaps, integrative phylogeographic approaches that combine molecular, morphological, and spatial data are needed (e.g., Koch et al., 2013; Scheriau et al., 2017), especially in groups affected by recent divergence and complex biogeographic histories.

Hypericum scruglii Bacch., Brullo & Salmeri represents an exemplary case of Mediterranean insular endemism. Originally described based on karyological, morphological and ecological criteria (Bacchetta et al., 2010), this species is endemic to Sardinia and occurs in specific habitats including temporary wetlands, springs, and pools. Molecular data on *H. scruglii* remain limited, with the species represented in the phylogenetic analysis of Nürk et al. (2013), but with insufficient sampling to resolve its evolutionary relationships fully. The taxonomic placement of *H. scruglii* within section *Adenosepalum* (Robson, 2016) is based on morphological affinities, particularly the presence of enlarged sepals and specific glandular patterns that characterize this section of approximately 30 species distributed across Europe and Asia (Bacchetta et al., 2010). Within this section, *H. scruglii* shows close morphological similarities with other Mediterranean taxa, particularly *H. tomentosum* L. and *H. pubescens* Boiss., both of which exhibit broader distributions across the western Mediterranean Basin. However, the evolutionary relationships among these species and the genetic basis of their morphological differentiation remain unclear.

Previous population genetic studies in *Hypericum* have provided valuable insights into species-level processes. Pilepić et al. (2011) investigated the genetic structure of *H. perforatum* using nuclear markers (but see also Scheriau et al., 2017) examined hybridization and polyploidy dynamics in the *H. perforatum*–*H. maculatum* complex, revealing significant gene flow between diploid and polyploid gene pools despite ecological differentiation. These studies highlight the importance of integrating multiple molecular markers and analytical approaches to understand complex evolutionary histories in this genus.

The integration of phylogenetic reconstruction with genealogical network analysis has proven particularly effective for resolving relationships among recently diverged lineages where traditional tree-based methods may lack resolution due to limited sequence divergence (Clement et al., 2000). In this framework, a genealogical network represents the mutational relationships among haplotypes or ribotypes, with nodes indicating each haplotype/ribotype and connections corresponding to single mutational steps, including hypothetical intermediates (median vectors) not observed in the dataset (Kholina et al., 2018). This approach is especially relevant for Mediterranean plant groups, where rapid diversification during Pleistocene climatic oscillations often resulted in shallow genetic divergences that are better captured by network-based methods than by bifurcating trees (De Castro et al., 2022).

The present study addresses these knowledge gaps by conducting a comprehensive molecular investigation of *H. scruglii* and its putative relatives within the Mediterranean *Adenosepalum* clade. Our specific objectives are to: (1) clarify the phylogenetic position of *H. scruglii* using an expanded molecular datasets; (2) assess genetic diversity and population structure across the three target species using both nuclear and plastid markers; (3) evaluate the extent of genetic differentiation between insular and continental populations; and (4) integrate phylogenetic and network-based approaches to elucidate patterns of evolutionary divergence in Mediterranean lineage. By combining newly generated sequence data with previously published datasets and employing comprehensive geographic sampling across species' ranges, this study provides a robust molecular framework for investigating patterns of diversification and divergence *Hypericum* and informing conservation strategies for insular endemics.

2. Materials and methods

2.1. Plant sampling

Field sampling was conducted across the natural distribution ranges of the three target species to ensure comprehensive geographic and genetic representation. For the endemic *H. scruglii*, four representative populations were sampled across its restricted Sardinia range (Italy). For the more widespread *H. tomentosum* and *H. pubescens*, sampling encompassed eight and five populations, respectively, spanning their distributions across Spain, France, Italy, and Malta. While our sampling does not encompass the entire distribution of each species, notably the Algerian range, it captures the principal insular and continental populations across the central Mediterranean. In total, 71 individuals from 17 populations were collected across Italy, Spain, France, and Malta, including insular systems from the Balearic Islands (BL), Sardinia (SA), Sicily (SI), and Malta (ME), thus covering four distinct Mediterranean biogeographic units (Fig. 1).

Sampling localities were selected to capture the full ecological and geographic range of each species while ensuring adequate population sizes for meaningful genetic analysis. North African populations were not included because collecting permits were not granted; therefore, the dataset reflects the European Mediterranean range. For each population, 3-8 individuals were sampled, maintaining minimum distances of 10 meters between individuals to avoid sampling clonal material. Fresh leaf tissue was collected in the field, desiccated in silica gel, and stored in a controlled-environment drying chamber (15°C, 15 % relative humidity) until DNA extraction. Voucher specimens were deposited at the Herbarium of the University of Cagliari (CAG) following standard herbarium protocols. Geographic coordinates for all sampling localities were recorded using GPS and are presented in Table S1. All field collections were carried out in collaboration with the GENMEDA seed-bank network, following its common ethical and sampling protocols (Bacchetta et al., 2008).

2.2. DNA extraction, amplification and sequencing

Total genomic DNA was extracted from approximately 20 mg of dried leaf tissue using the DNeasy Plant Mini Kit (Qiagen, Hilden, Germany) following the manufacturer's protocols with minor modifications. DNA quality and quantity were assessed using 1% agarose gel electrophoresis and spectrophotometric analysis (NanoDrop 2000, Thermo Fisher Scientific).

2.3. Marker selection and PCR amplification

Three molecular markers were selected based on their proven utility in *Hypericum* phylogenetics and population genetics (Meseguer et al., 2013; Scheriau et al., 2017): one nuclear ribosomal marker (complete ITS region: ITS1, 5.8S rRNA gene, ITS2) and two plastid intergenic spacers [*ycf*6-*psb*M and *trn*S$^{(GCU)}$–*trn*G$^{(UCC)}$]. These markers provide complementary evolutionary information, with the nuclear ITS region reflecting biparental inheritance and faster evolutionary rates, while the plastid markers represent uniparental (maternal) inheritance with more conservative evolutionary patterns.

PCR amplifications were performed in 25 µl reactions containing 1 × PCR buffer, 2.0 mM $MgCl_2$, 0.2 mM dNTPs, 0.4 µM of each primer, 1.0 U Taq DNA polymerase (Thermo Fisher Scientific), and approximately 20 ng template DNA. Primer sequences and thermal cycling conditions were adapted from established protocols. As nuclear markers (nrDNA), the ITS ribosomal cistron [Internal Transcribed Spacer 1 (ITS1), 5.8S

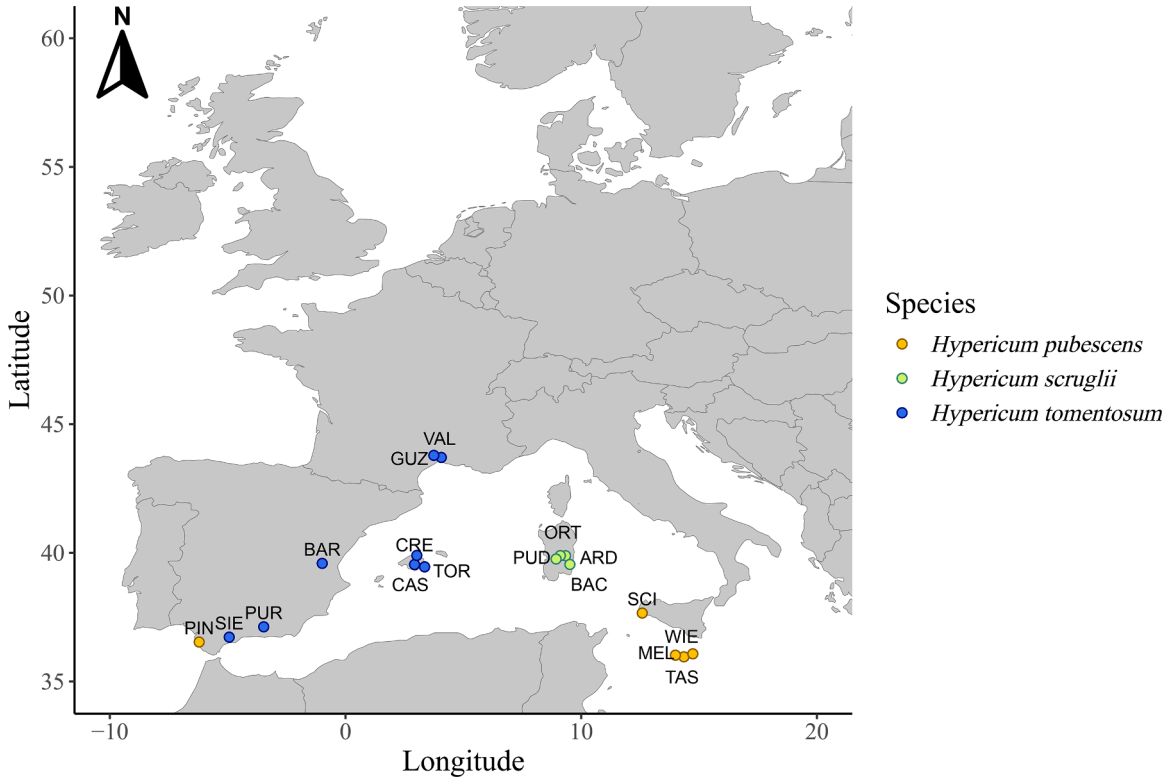

Fig. 1. Geographic distribution of the 17 sampled populations of *Hypericum scruglii, H. tomentosum*, and *H. pubescens* across the Mediterranean Basin, including Italy, France, Spain, and Malta. Each label corresponds to a population code used throughout the study: ARD, BAC, ORT, PUD, SCI (Italy); GUZ, VAL (France); CAS, CRE, BAR, PIN, PUR, SIE, TOR (Spain); MEL, TAS, WIE (Malta). The species *H. scruglii* was collected from ARD, BAC, ORT, and PUD. The species *H. tomentosum* was collected from GUZ, VAL, BAR, CAS, CRE, PUR, SIE, and TOR. Finally, the species *H. pubescens* was collected from SCI, MEL, TAS, WIE, and PIN. Coordinates are plotted in decimal degrees.

rRNA gene, Internal Transcribed Spacer 2 (ITS2)] was analysed using ITS1a/ITS4 primers (White et al., 1990; Aguilar et al., 1999) under cycling conditions of 94°C for 3 min, followed by 35 cycles of 94°C for 30 s, 55°C for 45 s, and 72°C for 60 s, with a final extension at 72°C for 5 min. Plastid markers (cpDNA) included the *trn*S$^{(GCU)}$–*trn*G$^{(UCC)}$ and *ycf*6–*psb*M intergenic spacers, with primer sequences and cycling conditions adapted from Hamilton (1999) and Shaw et al. (2007), respectively. PCR products were purified using ExoSAP-IT (USB Corporation) and sequenced in both directions using an ABI 3730xl DNA Analyzer (Applied Biosystems) at an external sequencing facility (Eurofins Genomics, Germany). Sequence chromatograms were assembled and edited using SeqAssem v.08/2004 (Hepperle, 2004), with manual verification of all polymorphic sites.

2.4. Sequence alignment and dataset preparation

Chromatograms were assembled and edited in SeqAssem (Hepperle, 2004). Multiple sequence alignments were generated with MAFFT v7 (Katoh and Standley, 2013) under the auto strategy and manually refined in MEGA11 (Tamura et al., 2021) to optimize gap placement and resolve ambiguous regions. The ITS dataset included 71 newly generated sequences, whereas plastid analyses were performed on 66 individuals for which both plastid spacers were successfully obtained and concatenated. To enhance phylogenetic resolution and provide broader taxonomic context, our 71 ITS sequences were combined with 317 previously published *Hypericum* ITS sequences retrieved from GenBank (Table S2), resulting in a total of 388 sequences. The final ITS alignment comprised 388 sequences with a total length of 633 bp after gap exclusion. The concatenated plastid alignment (*ycf*6–*psb*M + *trn*S$^{(GCU)}$–*trn*G$^{(UCC)}$) included 66 newly generated sequences plus 16 reference sequences from GenBank, for a total of 82 sequences with an aligned length of 1,300 bp. All newly generated sequences from this study have been deposited in GenBank (see Table S2 for the accession numbers). Taxonomic verification was performed using the Plants of the World Online database (Royal Botanic Gardens, Kew, POWO 2025) to ensure nomenclatural accuracy and resolve synonymies.

2.5. Data partitioning and congruence testing

Prior to combined analyses, we tested for incongruence between nuclear (ITS) and concatenated plastid datasets (*ycf*6–*psb*M + *trn*S$^{(GCU)}$–*trn*G$^{(UCC)}$) using the Partition Homogeneity Test (*PHT*) in PAUP* v4.0a (Swofford, 2003) with 1000 replicates. The complete dataset showed significant incongruence between the two genomic partitions ($p = 0.04$); therefore, concatenated analyses were not performed, and nuclear and plastid markers were analysed separately. Despite this statistical incongruence, phylogenetic analyses based on the focal dataset (three target species) recovered identical species-level topologies for nuclear and plastid data (Fig. 2A, 2B). A different topology involving the three focal species emerged only in the comprehensive ITS analysis including additional GenBank sequences (Fig. S1), indicating that apparent conflict at the focal lineage level arises only when broader taxon sampling is considered.

2.6. Phylogenetic analyses

Maximum Likelihood (ML) phylogenetic inference was conducted using IQ-TREE v2.1.2 (Minh et al., 2020). The best-fit substitution model was selected using ModelFinder (Kalyaanamoorthy et al., 2017) based on the Bayesian Information Criterion (BIC). This analysis identified the *GTR+F+I+G4* model as the best for both cpDNA and ITS datasets. Node support was evaluated using 1000 ultrafast bootstrap replicates

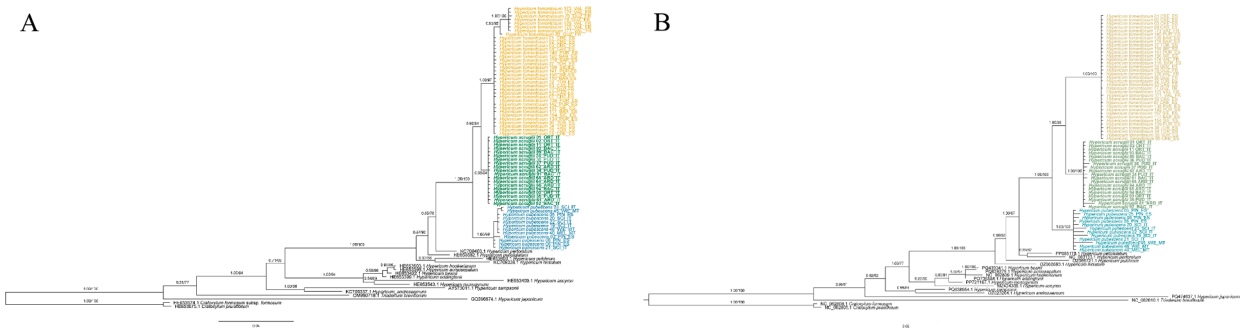

Fig. 2. Fig. 2. Maximum Likelihood (ML) phylogenetic trees with Bayesian posterior probability (PP) support values mapped onto nodes. (A) Nuclear ribosomal (ITS) phylogeny based on the 71 focal-species sequences. (B) Plastid phylogeny based on concatenated ycf6–psbM and trnS(GCU)–trnG(UCC) spacers. Support values are shown as PP/UFBoot; only values ≥0.80/80 are displayed. Trees were rooted with *Cratoxylum cochinchinense* and *C. formosum* following Nürk et al. (2013) and Scheriau et al. (2017). Species color codes: green = *H. scruglii*, blue = *H. tomentosum*, yellow/orange = *H. pubescens*.

(UFBoot; Hoang et al., 2018) and SH-aLRT replicates (Guindon et al., 2010). Bootstrap values ≥80% were considered indicative of strong support.

Bayesian Inference (BI) was performed using MrBayes v3.2.7 (Ronquist et al., 2012), applying the *GTR+I+G* model for both markers. Because nuclear (ITS) and plastid datasets represent independent genetic compartments, they were analysed separately, resulting in two independent Bayesian phylogenetic analyses (Fig. 2A and Fig. 2B). For each dataset, two independent Markov-chain Monte Carlo (MCMC) runs were performed, each consisting of four chains (one cold and three heated). For the cpDNA dataset, MCMC analyses were run for 15,000,000 generations, also sampling every 500 generations. To ensure robust convergence, the stop rule was enabled (stoprule=yes stopval=0.01 miniter=500000) and monitored via the average standard deviation of split frequencies (*ASDSF* < 0.01). Convergence diagnostics were verified in Tracer v1.7.1 (Rambaut et al., 2018), and all model parameters showed effective sample sizes (*ESS*) > 750, with LnPr, α, and tree length > 2,500. Burn-in was determined independently for each dataset based on convergence diagnostics. For the cpDNA dataset (Fig. 2B), convergence was reached rapidly and the first 4% of samples were discarded as burn-in. In contrast, the ITS dataset (Fig. 2A) showed slower stabilization of parameter estimates; therefore, the first 61.35% of samples were discarded as burn-in (average *SD* of split frequencies = 0.00968 ± 2.91 × 10^{-4}). A 50% majority-rule consensus trees were generated for both

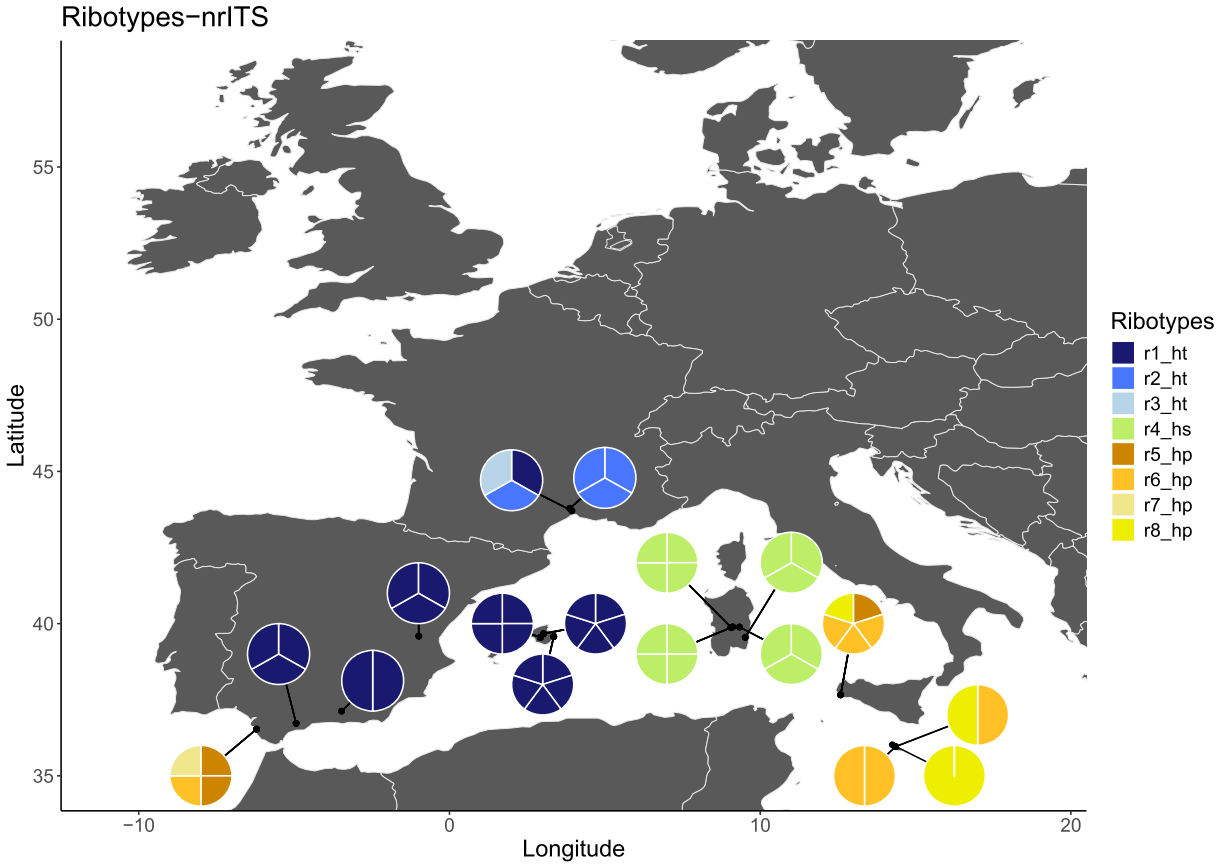

Fig. 3. Geographic distribution of nuclear ITS ribotypes across 17 Mediterranean populations of *Hypericum scruglii, H. tomentosum*, and *H. pubescens*. Each pie chart shows ribotype composition at each locality. Eight ribotypes were identified (r1–r8): r1–r3 (blue) occur in *H. tomentosum* populations in France and Spain; r4 (green) is exclusive to *H. scruglii* in Sardinia; r5–r8 (orange) occur in *H. pubescens* populations in Sicily, Malta, and Spain, with r6–r8 endemic to Malta. Population codes correspond to those in Fig. 1.

datasets, and posterior probability (*PP*) values were used to evaluate clade support. For outgroup rooting, we included a limited set of phylogenetically relevant taxa based on previous studies. Following Scheriau et al. (2017) and Nürk et al. (2013), we used *Cratoxylum cochinchinense* (Lour.) Blume and *C. formosum* (Jack) Benth. & Hook.f. ex Dyer as primary outgroups, which represent closely related genera within Hypericaceae and provide stable rooting for section Adenosepalum. Final trees were visualized and annotated using FigTree v1.4.4 (Rambaut, 2018) and graphically refined using Adobe Illustrator. To enhance interpretability, the ML tree was selected as the reference topology and Bayesian posterior probability (*PP*) values were manually mapped onto the ML topology, integrating both ML (*UFBoot*) and BI (*PP*) support values in a combined framework widely accepted in molecular systematics.

2.7. Genealogical network construction

Median-joining networks were constructed separately for nuclear and plastid datasets using the TCS algorithm implemented in PopART v1.7 (Leigh and Bryant, 2015). Node sizes were scaled by variant frequency, and missing intermediates were represented as inferred haplotypes (median vectors). Geographic distributions are illustrated in Fig. 3 and Fig. 4, whereas the corresponding network plots are shown in Fig. 5 (ITS) and Fig. 6 (cpDNA).

The ribotypes and the haplotypes identified by PopArt v1.7 (Leigh and Bryant, 2015) were subsequently plotted as scatterpie maps using the ggplot2 R package v.3.5.2. (Wickham, 2016). PopArt masks any columns in the alignment with gaps or ambiguous characters (?, N, Y, R) and remove sequences with more than 5% missing data.

For plastid data, indels were included as binary characters to maximize phylogenetic information content. Network nodes were scaled proportionally to ribotype/haplotype frequencies and missing intermediate ribotypes and haplotypes were represented as median vectors (inferred ancestral sequences). Geographic and taxonomic information was mapped onto networks to visualize spatial patterns of genetic diversity and identify potential dispersal routes or barriers to gene flow. The plastid network for *H. scruglii* was polarized (i.e., rooted using outgroup information) derived from the broader phylogenetic analysis to identify putative ancestral haplotypes and infer evolutionary directionality within the network (Clement et al., 2000). This approach provides valuable insights into colonization patterns and population history that may not be apparent from frequency data alone.

2.8. Population genetic analyses

Population genetic parameters were calculated using DnaSP v6 (Rozas et al., 2017). For each species and marker combination, we estimated nucleotide diversity (π), haplotype diversity (*Hd*), ribotype diversity (*nr*), and the number of segregating sites (*S*). Tajima's D statistic was calculated to test for departures from neutrality and demographic equilibrium.

Pairwise genetic differentiation among populations was quantified using Wright's *Fst* statistic calculated in Arlequin v3.5 (Excoffier and Lischer, 2010). Statistical significance was assessed using 10,000 permutations. *Fst* values were interpreted according to Wright's classification: 0-0.05 (little differentiation), 0.05-0.15 (moderate differentiation), 0.15-0.25 (great differentiation), and >0.25 (very great differentiation).

Analysis of Molecular Variance (AMOVA) was performed in Arlequin v3.5 to partition genetic variance among species, among populations within species, and within populations. Significance was tested using

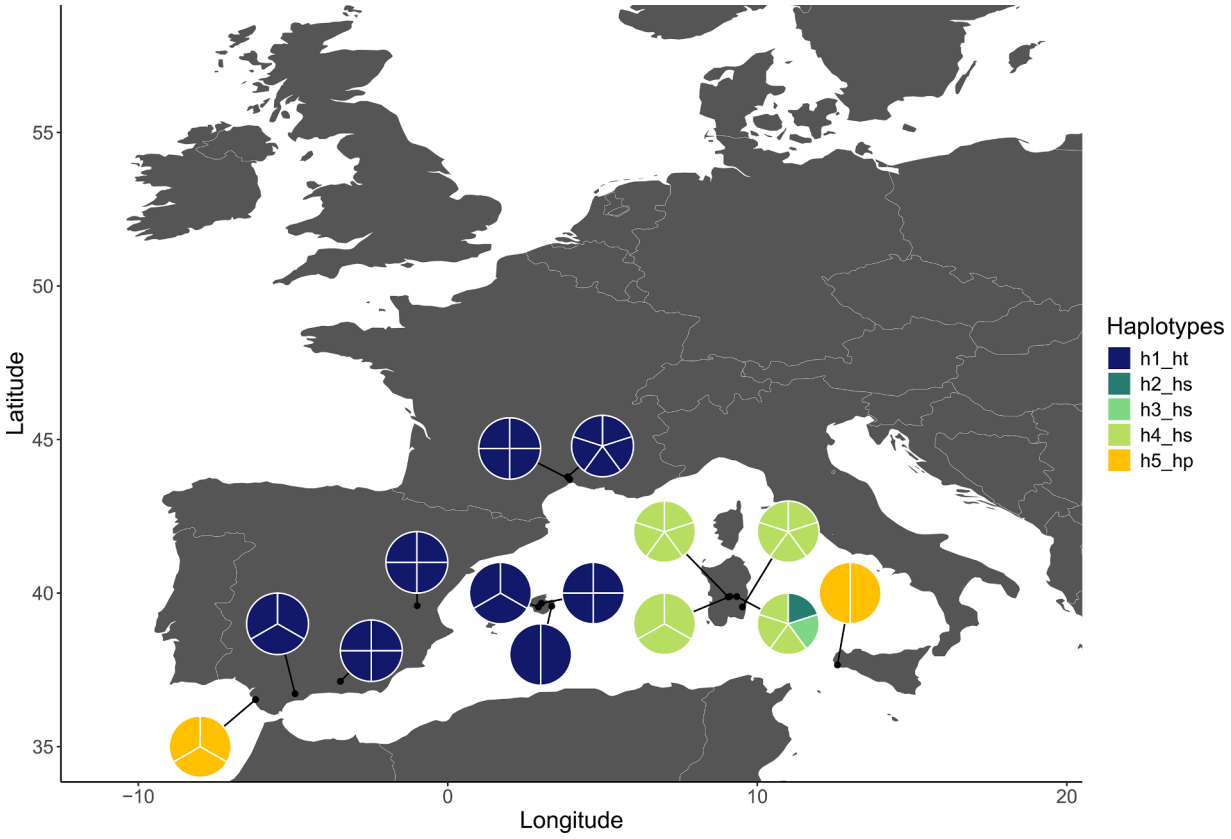

Fig. 4. Geographic distribution of plastid haplotypes [concatenated ycf6-psbM + trnS(GCU)–trnG(UCC)] across Mediterranean populations of *Hypericum scruglii, H. tomentosum*, and *H. pubescens*. Each pie chart shows haplotype composition at each locality. Five haplotypes were identified (h1–h5): h1 (dark blue) occurs in H. tomentosum populations in France and Spain; h2–h4 (green) are endemic to H. scruglii in Sardinia and closely related (1-2 mutations apart); h5 (orange) occurs in H. pubescens populations in Sicily and Spain. Population codes correspond to those in Fig. 1.

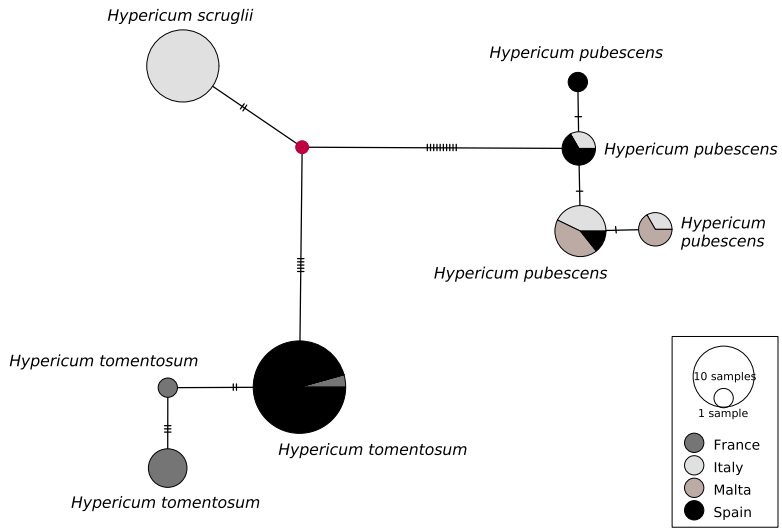

Fig. 5. Median-joining network of nuclear ITS ribotypes in *Hypericum scruglii, H. tomentosum* and *H. pubescens*. Circles represent ribotypes (r1–r8) and are scaled according to their frequency. Colors correspond to species: green = *H. scruglii*, blue = *H. tomentosum*, orange = *H. pubescens*. Lines represent single mutational steps; small black circles indicate inferred intermediate ribotypes (median vectors).

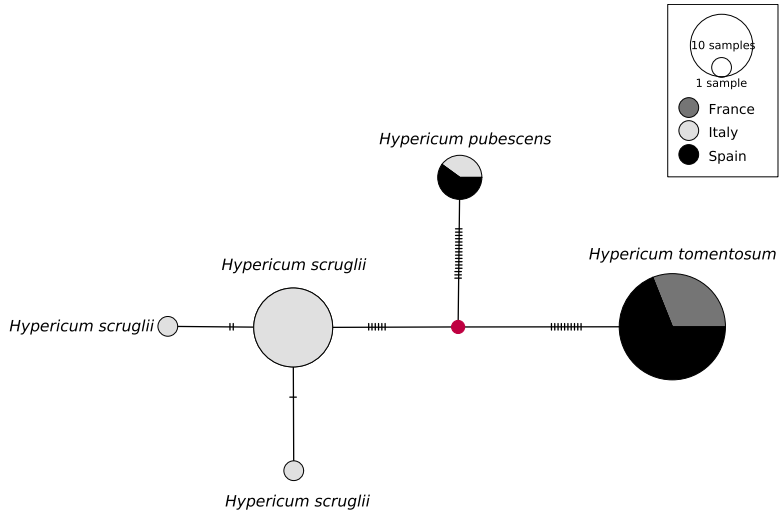

Fig. 6. Median-joining network of plastid haplotypes based on concatenated ycf6–psbM and trnS(GCU)–trnG(UCC) spacers. Circles represent haplotypes (h1–h5) and are scaled according to their frequency. Colors correspond to species as in Fig. 5. Lines represent single mutational steps; black dots indicate inferred intermediate haplotypes.

10,000 permutations.

3. Result

3.1. Congruence testing and phylogenetic incongruence

The Partition Homogeneity Test (*PHT*) revealed significant incongruence between nuclear and plastid datasets ($p = 0.04$). Robinson-Foulds topological distance analysis further quantified the incongruence in the complete dataset, with an average distance of 33.3 (range: 31.5-34.5, $SD \pm 0.53$) between consensus trees from the two datasets. This consistent level of topological conflict suggests systematic incongruence likely reflecting biological processes such as incomplete lineage sorting or historical introgression (Nürk et al., 2013, 2015), rather than stochastic variation. Given the documented cytonuclear discordance at multiple phylogenetic levels in *Hypericum* (Meseguer et al., 2013; Nürk et al., 2013, 2015), we conducted separate phylogenetic analyses for each genomic partition to accurately represent the evolutionary history of each marker system.

3.2. Phylogenetic relationships

Nuclear Phylogeny: the ITS tree (Fig. 2A) recovered *H. scruglii, H. tomentosum*, and *H. pubescens* as reciprocally monophyletic lineages with strong statistical support. Maximum Likelihood and Bayesian analyses yielded highly congruent topologies, with posterior probability/ultrafast bootstrap (*PP/UFBoot*) values of 0.96/94 for *H. scruglii*, 1.00/97 for *H. tomentosum*, and 1.00/99 for *H. pubescens*. While the majority of clades showed Bayesian Posterior Probabilities of $PP \geq 0.95$, a few nodes exhibited values in the range $PP = 0.86–0.94$, indicating variable levels of phylogenetic resolution.

The *H. scruglii* clade formed a strongly supported monophyletic group encompassing all Sardinian samples, confirming the genetic coherence of this endemic species. Within this clade, limited internal structure was observed, reflecting the recent divergence and restricted geographic distribution of the species. Relationships among the three

species were well-resolved, with *H. scruglii* and *H. tomentosum* forming a sister group relationship (*PP/UFBoot* = 0.94/92) that was sister to *H. pubescens* (*PP/UFBoot* = 1.00/100).

The comprehensive ITS analysis provided broader phylogenetic context but revealed a slightly different topology within the focal clade compared to the analysis with only our 71 newly generated sequences (Fig. 2A). Specifically, the comprehensive dataset recovered *H. scruglii* as sister to a clade containing *H. pubescens* + *H. tomentosum*, whereas our focal dataset (Fig. 2A) showed *H. pubescens* as sister to *H. scruglii* + *H. tomentosum*. This topological variation likely reflects the inclusion of additional taxa and the broader sampling scale, which can affect phylogenetic resolution in recently diverged groups. For the remainder of our analyses, we focus on relationships within our focal three-species dataset (Fig. 2), which provides higher resolution for the specific lineages under study.

Plastid Phylogeny: the plastid-based tree (Fig. 2B) recovered a generally similar species-level topology to the focal ITS analysis. All three target species formed well-supported monophyletic clades with maximum support values (PP/UFBoot = 1.00/100 for each species). The plastid phylogeny recovered *H. scruglii* and *H. tomentosum* as sister taxa with strong support (PP/UFBoot = 1.00/98), with *H. pubescens* forming the sister lineage to this clade.

This topology is congruent with the focal-species ITS analysis (Fig. 2A) at the species-level, with both datasets supporting *H. pubescens* as sister to the *H. scruglii* + *H. tomentosum* clade. However, topological conflict exists between the focal-species analysis (Fig. 2A) and the comprehensive ITS phylogeny (Fig. S1), which recovered *H. scruglii* as sister to *H. pubescens* + *H. tomentosum*. This discordance likely reflects the effects of increased taxon sampling on phylogenetic resolution in recently diverged lineages.

3.3. Nuclear (ITS) ribotype networks

Network analysis of ITS sequences revealed eight ribotypes distributed across the three species; their geographic distribution is shown in Fig. 3, while their separation by multiple mutational steps is illustrated in Fig. 5. *Hypericum scruglii* carried a single ribotype across four Sardinian populations (r4, Fig. 3 and 5), indicating low nuclear diversity likely reflecting recent insular colonization. *Hypericum tomentosum* displayed three ribotypes across eight populations from Spain and France (r1-r3, Fig. 3 and 5), whereas *Hypericum pubescens* showed the highest ribotype diversity among the three species, with four ribotypes across five populations (r5-r8, Fig. 3 and 5). Ribotype distribution showed a strong correspondence with species boundaries, as all ribotypes were species-specific and no ribotypes were shared among the three species. This pattern indicates clear nuclear differentiation among lineages. No ribotype differentiation was detected between Balearic and continental Spanish populations, whereas Sicilian populations shared ribotype r1 with other regions, while Maltese populations harbored private ribotypes (r2–r3), indicating a degree of differentiation between these two insular systems.

3.4. Plastid haplotype networks

The plastid network revealed five main haplotypes distributed across the three focal species; their geographic distribution is shown in Fig. 4, whereas their relationships are illustrated in Fig. 6. A well-defined Sardinian cluster was composed of three closely related haplotypes (h2-h4, Fig. 4 and 6), all detected exclusively in *H. scruglii* populations. The most common haplotype (h2) was shared across four populations, while h3 and h4 were separated from it by one and two mutational steps, respectively. Despite containing three haplotypes, *H. scruglii* showed lower overall plastid diversity (*Hd* = 0.58, π = 0.0008; see Section 3.5) than the other species, as these haplotypes are separated by very few mutations and show strongly unequal frequencies, with h2 being predominant. This pattern of reduced divergence and shared ancestral haplotype suggests recent and localized diversification of *H. scruglii* relative to the continental species. In contrast, the haplotype associated with *H. tomentosum* (h1) was distributed across Spanish and French populations. Similarly, the haplotype from *H. pubescens* (h5) was geographically structured groups, occurring in Sicilian populations, which represent the only confirmed Italian occurrences, and in Spain (Fig. 4).

3.5. Population genetic diversity

Genetic diversity parameters varied substantially among species and markers. Indeed, for the ITS region, *H. pubescens* exhibited the highest ribotype diversity (*Hd* = 0.78), followed by *H. tomentosum* (*Hd* = 0.65) and *H. scruglii* (*Hd* = 0.43). Nucleotide diversity followed a similar pattern, with *H. pubescens* showing the highest values (π = 0.0034) and *H. scruglii* the lowest (π = 0.0012). Plastid diversity showed consistently lower diversity values, with *H. scruglii* again exhibiting the lowest variation (*Hd* = 0.58, π = 0.0008). Tajima's D values were negative for all species-marker combinations but not statistically significant, suggesting demographic stability or mild population expansion.

3.6. Population differentiation and genetic structure

Pairwise *Fst* analyses revealed substantial genetic differentiation among populations, with plastid markers showing consistently higher differentiation than nuclear markers. Differentiation was strongest between Sardinian populations of *H. scruglii* and continental ones (plastid *Fst* > 0.60; nuclear *Fst* = 0.25-0.40), indicating moderate to strong divergence. Other insular populations (Balearic Islands, Sicily, Malta) also showed elevated differentiation from continental populations, although values were generally lower than those observed for Sardinia.

Within the continent, *H. tomentosum* and *H. pubescens* populations showed intermediate values (plastid *Fst* = 0.30-0.55; nuclear *Fst* = 0.15-0.35), suggesting limited but non-negligible gene flow among geographically proximate populations.

AMOVA results confirmed that the majority of genetic variation occurred among species (65.4% for plastid, 48.2% for nuclear markers), with substantial additional variation among populations within species (28.1% for plastid, 31.6% for nuclear). Within-population variation was lowest for plastid markers (6.5%) compared to nuclear ones (20.2%), reflecting the contrasting inheritance patterns and evolutionary dynamics of these genomic compartments.

4. Discussion

4.1. Phylogenetic relationships and species delimitation

Our comprehensive molecular analysis provides robust support for the taxonomic recognition of *H. scruglii* as a distinct species within section *Adenosepalum*. The consistent recovery of *H. scruglii* as a strongly supported monophyletic group in both nuclear and plastid analyses provides compelling evidence for its evolutionary independence. This molecular validation is particularly important given that the original species description was based primarily on karyological, morphological and ecological traits (Bacchetta et al., 2010), which can be subject to phenotypic plasticity and convergent evolution.

The sister-group relationship between *H. scruglii* and *H. tomentosum* revealed by nuclear phylogenetic analysis suggests a relatively recent divergence, possibly associated with the geological isolation of Sardinia starting with the Miocene opening of the Algerian Basin (Rosenbaum et al., 2002; Mansion et al., 2008; Meseguer et al., 2013). In addition, the substantial genetic differentiation observed (nuclear *Fst* > 0.25, plastid *Fst* > 0.60), combined with the complete geographic isolation and species-level monophyly, indicates that gene flow between these lineages has been effectively eliminated, allowing for independent evolutionary trajectories.

The phylogenetic position of *H. pubescens* as sister to the *H. scruglii*-*H. tomentosum* clade (Fig. 2) aligns with previous morphological assessments based on sepal and glandular characters (Bacchetta et al., 2010; Robson, 2016) and provides a framework for understanding the biogeographic history of this Mediterranean lineage. Further molecular dating analyses would be needed to establish the temporal sequence of divergence events within this clade.

4.2. Phylogeographic patterns and biogeographic history

The significant incongruence between nuclear and plastid phylogenies (*PHT, p*-value = 0.04) reflects complex evolutionary processes that are increasingly recognized as common in plant phylogeography. This pattern is most consistent with incomplete lineage sorting, where ancestral polymorphisms are retained across speciation events due to large effective population sizes and short divergence times relative to coalescent processes (Maddison, 1997; Li et al., 2021).

The geographic distribution of plastid haplotypes and ITS ribotypes provides insights into colonization patterns and population history. The concentration of genetic diversity in continental populations, particularly the high ITS ribotype diversity observed in *H. pubescens*, suggests that Mediterranean peninsulas served as glacial refugia during Pleistocene climatic oscillations, as similarly observed in *Cyperus esculentus* L. (De Castro et al., 2015).

The phylogeographic structure revealed in network analyses, with Sardinian haplotypes forming a distinct cluster connected to continental haplotypes by multiple mutational steps, supports a colonization scenario where Sardinia was colonized from continental sources, followed by in situ divergence and the evolution of *H. scruglii* as an endemic species. Indeed, the restricted plastid variation of *H. scruglii*, dominated by a single widespread haplotype with only two minor derivatives, points to its recent insular origin and comparatively shallow evolutionary history. The complete allopatry of plastid haplotypes among the three species, despite extensive sampling across the Mediterranean Basin, strongly supports limited historical gene flow and reinforces the genetic distinctiveness of each species. This pattern indicates that the Strait of Messina and broader Mediterranean Sea have served as effective barriers to gene flow, promoting allopatric divergence among island and continental lineages. A contrasting scenario is observed in *Cyperus esculentus*, where haplotypes are widely distributed across Europe despite strong geographic structure, reflecting both its invasive ecology and capacity for long-distance dispersal through both natural and human-mediated processes (De Castro et al., 2015; Follak et al., 2016). Unlike Cyperus, which exhibits high dispersal capacity and ecological plasticity, *Hypericum* species in section Adenosepalum show limited seed dispersal across marine barriers, as evidenced by the complete allopatric distribution of plastid haplotypes. This contrast emphasizes how differences in life-history traits and dispersal mechanisms shape phylogeographic patterns. Taken together, these results highlight the pivotal role of geographic barriers in shaping the phylogeographic structure of Mediterranean *Hypericum*. In this context, the distribution of ribotypes in *H. tomentosum*, with one shared across France and Spain and another confined to France, suggests higher ribotype diversity in French populations compared to Iberian ones, consistent with the Pyrenees acting as a biogeographic barrier, a role previously documented for other plant lineages (Charrier et al., 2014; Listl et al., 2017).

4.3. Conservation implications

Our results have direct implications for the conservation of Mediterranean *Hypericum* diversity, particularly for the endemic *H. scruglii*. The genetic distinctiveness of this species, combined with its restricted geographic distribution, places it at high risk of extinction due to habitat loss, climate change, or stochastic events (e.g. De Castro et al. 2025), in agreement with its current IUCN Red List assessment as Endangered, based on restricted distribution, habitat degradation and population decline (Fois et al., 2014).

Specific conservation priorities: (1) Population Protection: All four sampled *H. scruglii* populations should receive immediate protection status, as they harbor distinct genetic variants that represent the full spectrum of evolutionary diversity within the species. (2) *Habitat Conservation*: Priority should be given to protecting the specific ecological conditions that support *H. scruglii* populations, including temporary wetlands, springs, and pools that are highly vulnerable to human alteration of hydrological regimes and to ongoing climate change. (3) *Ex situ conservation*: the species' narrow range and vulnerability underline the importance of seed banking and cultivation protocols. Six accessions from four populations are currently safeguarded in the Sardinian Germplasm Bank (BG-SAR), with duplicates stored at the Millennium Seed Bank of the Royal Botanic Gardens, thereby ensuring long-term preservation (Porceddu et al., 2020). (4) *Population Monitoring:* Regular monitoring of population sizes and demographic parameters is recommended to detect early signs of decline and inform adaptive management strategies.

Plastid markers revealed strong differentiation of Sardinian populations of *H. scruglii* compared to both continental and other insular populations, whereas nuclear markers indicated more moderate levels of divergence. This pattern suggests very limited seed-mediated gene flow, with occasional pollen-mediated dispersal across longer distances. It has important implications for natural population dynamics and conservation planning. Nevertheless, long-term safeguarding of *H. scruglii* will require sustained regional resources, which are currently lacking, to secure both in situ and ex situ conservation actions.

The contrasting patterns between plastid (*Fst* > 0.60) and nuclear markers (*Fst* = 0.25-0.40) suggest that while seed-mediated gene flow is essentially absent across marine barriers, occasional pollen-mediated gene exchange may occur over longer distances. This interpretation is consistent with the more restricted dispersal capability of seeds compared to pollen in animal-pollinated *Hypericum* species (Nürk et al., 2013). Field observations suggest that *H. scruglii* populations are small (typically <500 reproductive individuals; Fois et al., 2014) and fragmented, with the species restricted to specialized habitats vulnerable to hydrological changes. These demographic characteristics, combined with its narrow geographic range, heighten extinction risk under current climate change scenarios (Porceddu et al., 2020).

4.4. Methodological advances and broader applications

Our study demonstrates the value of combining multiple analytical methods to resolve evolutionary relationships in recently diverged Mediterranean lineages. While phylogenetic tree reconstruction provided strong support for species-level monophyly, network analyses revealed finer-scale phylogeographic structure and identified putative ancestral haplotypes through topology and frequency distributions. The incongruence detected between nuclear and plastid markers underscores the importance of sampling multiple independent genetic compartments, as each provides complementary information on evolutionary history. The use of outgroup information to infer directionality in networks (following Clement et al., 2000) proved particularly valuable for reconstructing colonization patterns, allowing us to distinguish between ancestral and derived haplotypes within the Sardinian endemic *H. scruglii.*

4.5. Future research directions

Future studies should focus on expanding genomic resources through next-generation sequencing approaches. Population genomic studies using reduced-representation sequencing (e.g., Restriction site Associated DNA sequencing (RAD-seq), Genotyping-by-Sequencing (GBS) or whole-genome resequencing) would provide higher resolution for detecting recent demographic events, quantifying gene flow, and identifying adaptive genetic variation. The integration of ecological niche

modelling with phylogeographic data would provide additional insights into the environmental factors driving diversification and the potential impacts of climate change on species distributions. This approach would be especially relevant for predicting the future persistence of endemic species like *H. scruglii* under projected climate scenarios.

5. Conclusions

This study provides a molecular phylogenetic and phylogeographic analysis of three Mediterranean *Hypericum* species, with particular focus on the Sardinian endemic *H. scruglii*. Our results demonstrate strong support for the taxonomic distinctiveness of *H. scruglii* based on both nuclear and plastid molecular markers, validating its species-level recognition and endemic status. Moreover, complex evolutionary relationships characterized by significant incongruence between nuclear and plastid phylogenies, indicating incomplete lineage sorting and highlighting the importance of using multiple molecular markers in phylogenetic studies.

Clear geographic structuring of genetic diversity, with complete allopatry among species and strong differentiation between insular and continental populations, supporting limited historical gene flow across the Mediterranean Basin. Effective application of network-based approaches to complement traditional phylogenetic methods, particularly for recently diverged lineages where sequence divergence is limited. These findings contribute to our understanding of plant diversification in the Mediterranean Basin and provide a robust framework for future research on *Hypericum* systematics and evolution. The molecular resources and analytical approaches developed in this study will facilitate ongoing conservation efforts and support the sustainable management of Mediterranean plant diversity in the face of increasing environmental pressures.

Funding

This research was funded by NANOFITOCARE, PSR 2007-2013 REG. (CE) N.1698/2005-MISURA 124 - Cooperazione per lo sviluppo di nuovi prodotti, processi e tecnologie nei settori agricolo e alimentare in quello forestale (Det. n. 4230/14, 27/08/2014), Italy.

CRediT authorship contribution statement

Veronica Malavasi: Writing – review & editing, Writing – original draft, Software, Methodology, Formal analysis, Data curation, Conceptualization. **Núria Beltran-Sanz:** Writing – review & editing, Writing – original draft, Software, Methodology, Formal analysis, Data curation, Conceptualization. **Caterina Angela Dettori:** Writing – review & editing, Conceptualization. **Olga De Castro:** Writing – review & editing, Supervision, Methodology, Data curation, Conceptualization. **Gianluigi Bacchetta:** Writing – review & editing, Supervision, Investigation, Conceptualization.

Declaration of competing interest

The authors declare that they have no known competing financial interests or personal relationships that could have appeared to influence the work reported in this paper.

Aknowledgements

We are grateful to the Germplasm Banks of the CIEF (Valencia), Jardí Botànic de Sóller, CBNM of Porquerolles, the University of Catania, and the Argotti Botanical Museum of Malta for their valuable support in providing plant material and assistance with conservation activities. We sincerely thank S. Brullo, E. Laguna, M. Porceddu, M. Vicens, S. Mifsud, P. Ferrer, F.B. Navarro, L. Scuderi, K. Diadema, J. Cursach, C. Cardona, J. Thompson, J.M. Vergara, A. Mateu, M.N. Jiménez, E.M. Cañadas, M. Guerrero, J.M. Fuentes Carretes, M. Boi, L. Serreli, and M. Orrù for their essential help during fieldwork, sampling, and data collection. Finally, we sincerely thank the two reviewers for their helpful and constructive suggestions, in particular Dr. Nicolai Nürk and an anonymous reviewer, which greatly improved the previous version of this manuscript.

Supplementary materials

Supplementary material associated with this article can be found, in the online version, at doi:10.1016/j.flora.2026.152945.

Data availability

Data will be made available on request.

References

Aguilar, J.F., Rosselló, J.A., Feliner, G.N., 1999. Nuclear ribosomal DNA (nrDNA) concerted evolution in natural and artificial hybrids of Armeria (Plumbaginaceae). Mol. Ecol. 8, 1341–1346.

Al-Khayri, J.M., Wudeli, S., Vennapusa, A.R., Nagella, P., Shehata, W., Al-Mssallem, M., 2024. Biotechnological approaches for the production of hypericin and other important metabolites from the genus *Hypericum*. Plant Cell Tiss. Organ Cult. 156 (3), 100. https://doi.org/10.1007/s11240-024-02723-7.

Allaw, M., Manconi, M., Aroffu, M., Marongiu, F., Porceddu, M., Bacchetta, G., Usach, I., Rached, R.A., Rajha, H.N., Maroun, R.G., Pedraz, J.L., Lopez-Mendez, T.B., Fadda, A. M., Manca, M.L., 2020. Extraction, characterization and incorporation of *Hypericum scruglii* extract in ad hoc formulated phospholipid vesicles designed for the treatment of skin diseases connected with oxidative stress. Pharmaceutics 12 (11), 1010. https://doi.org/10.3390/pharmaceutics12111010.

Bacchetta, G., Bueno Sánchez, A., Fenu, G., Jiménez-Alfaro, B., Mattana, E., Piotto, B., Virevaire, M. (Eds.), 2008. Conservación *ex situ* de plantas silvestres. Principado de Asturias /La Caixa, Oviedo, p. 378.

Bacchetta, G., Brullo, S., Salmeri, C., 2010. *Hypericum scruglii* sp. nov. (Guttiferae) from Sardinia. Nord. J. Bot. 28 (4), 469–474.

Bacchetta, G., Farris, E., Pontecorvo, C., 2012. A new method to set conservation priorities in biodiversity hotspots. Plant Biosyst 146, 638–648. https://doi.org/10.1080/11263504.2011.642417.

Cañadas, E.M., Fenu, G., Peñas, J., Lorite, J., Mattana, E., Bacchetta, G., 2014. Hotspots within hotspots: endemic plant richness, environmental drivers, and implications for conservation. Biol. Conserv. 170, 282–291.

Charrier, O., Dupont, P., Pornon, A., Escaravage, N., 2014. Microsatellite marker analysis reveals the complex phylogeographic history of *Rhododendron ferrugineum* (Ericaceae) in the Pyrenees. PLoS One 9 (4), e92976.

Clement, M., Posada, D., Crandall, K.A., 2000. TCS: a computer program to estimate gene genealogies. Mol. Ecol. 9, 1657–1659.

Crockett, S.L., Robson, N.K.B., 2011. Taxonomy and chemotaxonomy of the genus *Hypericum*. Medicin. Aromat. Plant Sci. Biotechnol. 5 (1), 1–13.

De Castro, O., Gargiulo, R., Del Guacchio, E., Caputo, P., De Luca, P., 2015. A molecular survey concerning the origin of *Cyperus esculentus* (Cyperaceae, Poales): two sides of the same coin—weed vs. Crop. Ann. Bot. 115 (2), 189–201. https://doi.org/10.1093/aob/mcu226.

De Castro, O., Bacchetta, G., Brullo, S., Del Guacchio, E., Di Iorio, E., Piazza, C., Caputo, P., 2022. Variability and nativeness in the Mediterranean taxa: divergence and phylogeography of *Genista etnensis* (Fabaceae) inferred from nuclear and plastid data. Plants 11, 3171. https://doi.org/10.3390/plants11223171.

De Castro, O., Piazza, C., Di Iorio, E., Bacchetta, G., Menale, B., 2025. Impact of barriers on Cyrno-Sardinian endemisms: a comparative study of population genetics and phylogeography within taxa of *Centranthus* sect. *Nervosae* (Caprifoliaceae). Plant Biol 27 (3), 362–377. https://doi.org/10.1111/plb.13775.

Excoffier, L., Lischer, H.E., 2010. Arlequin suite ver 3.5: a new series of programs to perform population genetics analyses under Linux and Windows. Mol. Ecol. Resour. 10, 564–567.

Fois, M., Cuena, A., Fenu, G., Bacchetta, G., 2014. *Hypericum scruglii* Bacch., Brullo et Salmeri. Inform. Bot. Ital. 46 (2), 308–310.

Follak, S., Belz, R., Bohren, C., Castro, O.D., Guacchio, E.D., Pascual-Seva, N., Schwarz, M., 2016. Biological flora of central Europe: *cyperus esculentus* L. Perspect. Plant Ecol., Evol. Syst. 23, 33–51. https://doi.org/10.1016/j.ppees.2016.09.003.

Guindon, S., Dufayard, J.F., Lefort, V., Anisimova, M., Hordijk, W., Gascuel, O., 2010. New algorithms and methods to estimate maximum-likelihood phylogenies: assessing the performance of PhyML 3.0. Syst. Biol. 59, 307–321.

Hamilton, M.B., 1999. Four primer pairs for the amplification of chloroplast intergenic regions with intraspecific variation. Mol. Ecol. 8, 521–523.

Hepperle, D., 2004. SeqAssem, Version 08/2004: view, edit, proofread & assemble molecular sequence & trace data. http://wwwuser.gwdg.de/~dhepper/seqassem/ accessed June 2025.

Hoang, D.T., Chernomor, O., von Haeseler, A., Minh, B.Q., Vinh, L.S., 2018. UFBoot2: improving the ultrafast bootstrap approximation. Mol. Biol. Evol. 35, 518–522.

Kalcev, G., Testa, G., Manconi, M., Bacchetta, G., Scano, A., Orrù, G., Deidda, M.C., Finco, G., Carta, M.G., 2021. *Hypericum scruglii* Bacch., Brullo & Salmeri, a potential

natural remedy for fibromyalgia: a narrative review. Biointerface Res. Appl. Chem. 11 (3), 9928–9938. https://doi.org/10.33263/BRIAC113.99289938.
Kalyaanamoorthy, S., Minh, B.Q., Wong, T.K.F., von Haeseler, A., Jermiin, L.S., 2017. ModelFinder: fast model selection for accurate phylogenetic estimates. Nat. Methods 14 (6), 587–589. https://doi.org/10.1038/nmeth.4285.
Katoh, K., Standley, D.M., 2013. MAFFT multiple sequence alignment software version 7: improvements in performance and usability. Mol. Biol. Evol. 30 (4), 772–780. https://doi.org/10.1093/molbev/mst010.
Kholina, A.B., Kozyrenko, M.M., Artyukova, E.V., et al., 2018. Modern state of populations of endemic *Oxytropis* species from baikal siberia and their phylogenetic relationships based on chloroplast DNA markers. Russ. J. Genet. 54, 805–815.
Kitanov, G.M., 2001. Hypericin and pseudohypericin in some *Hypericum* species. Biochem. Syst. Ecol. 29, 171–178. https://doi.org/10.1016/S0305-1978(00)00032-6.
Koch, M.A., Scheriau, C., Betzin, A., Hohmann, N., Sharbel, T.F., 2013. Evolution of cryptic gene pools in *Hypericum perforatum*: the influence of reproductive system and gene flow. Ann. Bot. 111, 1083–1094.
Leigh, J.W., Bryant, D., 2015. POPART: full-feature software for haplotype network construction. Methods Ecol. Evol. 6, 1110–1116.
Li, H.T., Luo, Y., Gan, L., Ma, P.-F., Gao, L.M., Yang, J.B., Cai, J., Gitzendanner, M.A., Fritsch, P.W., Zhang, T., Jin, J.J., Zeng, C.X., Wang, H., Yu, W.B., Zhang, R., van der Bank, M., Olmstead, R.G., Hollingsworth, P.M., Chase, M.W., Soltis, D.E., Soltis, P.S., Yi, T.S., Li, D.Z., 2021. Plastid phylogenomic insights into relationships of all flowering plant families. BMC Biol 19, 232. https://doi.org/10.1186/s12915-021-01166-2.
Listl, D., Poschlod, P., Reisch, C., 2017. Phylogeography of a tough rock survivor in European dry grasslands. PLoS One. 12 (6), e0179961.
Maddison, W.P., 1997. Gene trees in species trees. Syst. Biol. 46, 523–536.
Mansion, G., Rosenbaum, G., Schoenenberger, N., Bacchetta, G., Rosselló, J.A., Conti, E., 2008. Phylogenetic analysis informed by geological history supports multiple, sequential invasions of the Mediterranean basin by the angiosperm family Araceae. Syst. Biol. 57, 269–285. https://doi.org/10.1080/10635150802044029.
Meseguer, A.S., Aldasoro, J.J., Sanmartin, I., 2013. Bayesian inference of phylogeny, morphology and range evolution reveals a complex evolutionary history in St. John's Wort (*Hypericum*). Mol. Phylogenet. Evol. 67, 379–403.
Minh, B.Q., Schmidt, H.A., Chernomor, O., Schrempf, D., Woodhams, M.D., von Haeseler, A., Lanfear, R., 2020. IQ-TREE 2: New models and efficient methods for phylogenetic inference in the genomic era. Mol. Biol. Evol. 37, 1530–1534. https://doi.org/10.1093/molbev/msaa015.
Nürk, N.M., Madrinán, S., Carine, M.A., Chase, M.W., Blattner, F.R., 2013. Molecular phylogenetics and morphological evolution of St. John's Wort (*Hypericum*; Hypericaceae). Mol. Phylogenet. Evol. 66, 1–16.
Nürk, N.M., Uribe-Convers, S., Gehrke, B., Tank, D.C., Blattner, F.R., 2015. Oligocene niche shift, miocene diversification-cold tolerance and accelerated speciation rates in the St. John's Worts (*Hypericum*, Hypericaceae). BMC Evolution. Biol. 15 (1), 80. https://doi.org/10.1186/s12862-015-0359-4.
Pilepić, K.H., Balić, M., Blažina, N., 2011. Estimation of phylogenetic relationships among some *Hypericum* (Hypericaceae) species using internal transcribed spacer sequences. Plant Biosyst 145 (1), 81–87.
Porceddu, M., Sanna, M., Serra, S., Manconi, M., Bacchetta, G., 2020. Seed germination requirements of *Hypericum scruglii*, an endangered medicinal plant species of Sardinia (Italy). Botany 98 (10), 615–621. https://doi.org/10.1139/cjb-2020-0039.
POWO, 2025. Facilitated by the Royal Botanic Gardens. Plants of the World Online, Kew. Published on the Internet. https://powo.science.kew.org/ (accessed 12 August 2025).
Rambaut, A., 2018. FigTree v1.4.4: tree figure drawing tool. http://tree.bio.ed.ac.uk/software/figtree/ accessed August 2025.
Robson, N.K.B., 1981. Studies in the genus *Hypericum* L. (Guttiferae). 2. Charact. Genus Bull. Br. Mus. Nat. Hist. (Bot.) 8, 55–226.
Robson, N.K.B., 2003. *Hypericum* botany. In: Ernst, E. (Ed.), Hypericum: the genus *Hypericum*. Taylor and Francis, London, pp. 1–22.
Robson, N.K.B., 2006. Studies in the genus *Hypericum* L. (Clusiaceae). Section 9. *Hypericum* sensu lato (part 3): subsection 1. *Hypericum* series 2. *Senanensia*, subsection 2. Erecta and section 9b. *Graveolentia*. Systemat. Biodiversity 4 (1), 19–98.
Robson, N.K.B., 2016. And then came molecular phylogenetics–reactions to a monographic study of *Hypericum* (Hypericaceae). Phytotaxa 255 (3), 181–198. https://doi.org/10.11646/phytotaxa.255.3.1.
Ronquist, F., Teslenko, M., van der Mark, P., Ayres, D.L., Darling, A., Höhna, S., Larget, B., Liu, L., Suchard, M.A., Huelsenbeck, J.P., 2012. MrBayes 3.2: efficient Bayesian phylogenetic inference and model choice across a large model space. Syst. Biol. 61 (3), 539–542.
Rosenbaum, G., Lister, G.S., Duboz, C., 2002. Reconstruction of the tectonic evolution of the western Mediterranean since the Oligocene. J. Virtual Explor. 8, 107–130.
Rozas, J., Ferrer-Mata, A., Sánchez-DelBarrio, J.C., Guirao-Rico, S., Librado, P., Ramos-Onsins, S.E., Sánchez-Gracia, A., 2017. DnaSP 6: DNA sequence polymorphism analysis of large data sets. Mol. Bio. Evol. 34 (12), 3299–3302.
Scheriau, C.L., Nuerk, N.M., Sharbel, T.F., Koch, M.A., 2017. Cryptic gene pools in the *Hypericum perforatum–H. maculatum* complex: diploid persistence versus trapped polyploid melting. Ann. Bot. 120, 955–966. https://doi.org/10.1093/aob/mcx110.
Shaw, J., Lickey, E.B., Schilling, E.E., Small, R.L., 2007. Comparison of whole chloroplast genome sequences to choose noncoding regions for phylogenetic studies in angiosperms: the tortoise and the hare III. Am. J. Bot. 94, 275–288.
Swofford, D.L., 2003. PAUP*. Phylogenetic Analysis Using Parsimony (*and Other Methods). Version 4. SinauerAssociates, Sunderland, Massachusetts.
Tamura, K., Stecher, G., Kumar, S., 2021. MEGA11: molecular evolutionary genetics analysis version 11. Mol. Biol. Evol. 38, 3022–3027.
White, T.J., Bruns, T., Lee, S., Taylor, J., 1990. Amplification and direct sequencing of fungal ribosomal RNA genes for phylogenetics. In: Innis, M.A., Gelfand, D.H., Sninsky, J.J., White, T.J. (Eds.), PCR Protocols: A Guide to Methods and Applications. Academic Press, San Diego, pp. 315–321.
Wickham, H., 2016. ggplot2: elegant graphics for data analysis. Springer-Verlag, New York. ISBN 978-3-319-24277-4. https://ggplot2.tidyverse.org.